Desalination and Water Treatment
www.deswater.com
doi: 10.1080/19443994.2015.1021849

57 (2016) 8437–8446
April

Taylor & Francis
Taylor & Francis Group

Continuous adsorption study of congo red using tea waste in a fixed-bed column

Mohammad Foroughi-dahr[a], Mohamad Esmaieli[a,b,*], Hossein Abolghasemi[a], Alireza Shojamoradi[a], Ehsan Sadeghi Pouya[a]

[a]*Center for Separation Processes Modeling and Nano-Computations, School of Chemical Engineering, College of Engineering, University of Tehran, 11365-4563, Tehran, Iran, emails: mfd.foroughi@gmail.com, mfd.foroughi@ut.ac.ir (M. Foroughi-dahr), Tel. +9821 61113617; Fax: +9821 66954051; emails: esmaili@ut.ac.ir (M. Esmaieli), hoab@ut.ac.ir (H. Abolghasemi), a.shoja@ut.ac.ir (A. Shojamoradi), sadeghipouya@ut.ac.ir (E. Sadeghi Pouya)*
[b]*Oil and Gas Center of Excellence, University of Tehran, Tehran, Iran*

Received 15 July 2014; Accepted 11 February 2015

ABSTRACT

In this paper, continuous fixed-bed studies were carried out to investigate the feasibility of using tea waste (TW) as a low-cost adsorbent for the removal of Congo red (CR) from aqueous solution. Effects of various parameters, such as mass of the adsorbent, flow rate, influent dye concentration, and initial pH were investigated. It was found that the amount of the column adsorption capacity was at about 3 mg/g. Three commonest models, namely Adams–Bohart, Thomas, and Yoon–Nelson models have been employed to predict the adsorption breakthrough curves of CR onto TW. The Adams–Bohart model satisfactorily predicts the initial parts of the adsorption process with the correlation coefficient at about 0.9. The Thomas and Yoon–Nelson models were found to be in reasonable agreement with the experimental data. In addition, the bed depth service time (BDST) model was applied at different bed depths. The results revealed that the experimental data greatly described using BDST model. It was concluded that the fixed-bed adsorption column with TW adsorbent can be used as a wastewater treatment for the removal of CR.

Keywords: Tea waste; Congo red; Adsorption; Fixed-bed column; Breakthrough curve

1. Introduction

Nowadays, the industrial discharge is a major concern. Dyes are the most undesirable pollutants contained in various industries, particularly textile industries. The presence of even a small quantity of dyes in water is highly visible and undesirable [1]. Dyes affect the aquatic systems, since they reduce the sunlight transmission through water and they may cause severe damage to human and animal health [2]. Most of the dyes are synthetic compounds with complex aromatic structures, which make them stable and difficult to be biodegraded. Various treatment processes, including adsorption, coagulation, ozonation, and membrane have been developed as an alternative to remove dye molecules from aqueous solutions [3]. It is observed that adsorption is an effective process for the removal of dyes from aqueous solution because of its simplicity as well as the availability of a wide range of adsorbent. Activated carbon is the most common

*Corresponding author.

adsorbent for the removal of dyes with high adsorption capacity [4,5]. However, its high price and difficulties of regeneration restrict the use of activated carbon as an adsorbent. Economically, the adsorption process depends on the adsorbent price. Therefore, it is preferred to employ low-cost adsorbents [6]. Recently, there have been several investigations on finding favorable adsorbents as cattail root [7], pine cone [8], red mud [9], and rice husk [10] for the removal of Congo red (CR) from aqueous solutions. CR is a benzidine-based anionic diazo dye which is known to cause allergic reactions. The azo dyes are characterized by the presence of at least one azo group consisting of nitrogen–nitrogen double bonds.

There are many researches on the batch adsorption for the removal of dyes reported in the literature. It is conducted to evaluate the possibility of the adsorbent for the removal of dye as an adsorbate. The batch experiments can easily be used in the laboratory for the treatment of small volumes of effluents, however are not useful in the case of column-mode operations. According to industrial point of view, the continuous flow adsorption in the fixed-bed column is more convenient [11]. It provides precious information for the adsorption reactor scale up as well as adsorption dynamic simulation [12]. The bench-scale column testing will result the adsorption breakthrough curves which can be exploited to design and operate fixed-bed adsorption plants. Both the transport processes in the column and in the adsorbent may influence the shape of the breakthrough curves. The breakthrough curves determine the bed height and the operating lifespan of the bed and regeneration times [13,14].

The tea plants are commonly cultivated in the northern area of Iran. Tea waste (TW) has been employed for the removal of several heavy metals and dyes from aqueous solutions [15–17]. In our previous study, TW was used as an adsorbent for the removal of CR in batch mode experiments and the effects of different parameters were investigated [15]. The resulted experimental data revealed that TW can be used as a potential adsorbent for the removal of CR with greater adsorption capacity with respect to the other natural adsorbents.

Recently, TW has been used in fixed-bed adsorption processes for the removal of pollutants, particularly heavy metals such as Pb(II), Ni(II), and Cr(VI) [18–20]. However, to the best of our knowledge, little attention has been paid to the fixed-bed adsorption of dyes with TW adsorbent. There are several models, including Adams–Bohart [21], Thomas [22], Yoon–Nelson [23], and BDST [24] for predicting the fixed-bed adsorption processes.

The objective of this study was to investigate the removal efficiency of TW for the removal of CR from aqueous solution in a fixed-bed column. The effects of design parameters, such as initial dye concentration, pH of the solution, flow rate, and bed depth on the adsorption of CR were studied using a laboratory-scale fixed-bed column. The Adams–Bohart, Thomas, Yoon–Nelson, and BDST models were used to analyze and predict the breakthrough curves for the adsorption of CR.

2. Experimental

2.1. Adsorbate

CR [1-naphthalene sulfonic acid, 3,30-(4,40-biphenylenebis (azo)) bis (4-amino) disodium salt] used in this study was supplied by Merck company. Its C.I. No. is 22120, FW = 696, chemical formula = $C_{32}H_{22}N_6Na_2O_6S_2$, and λ_{max} = 495 nm. The molecular structure of CR is illustrated in Fig. 1.

2.2. Preparation of adsorbent

Tea leaves used in this experiment were produced in tea plantations from the northern area of Iran. The TW was collected and prior to the experiments, it was washed with tap water several times to remove all dirt and dye particles. It was continued until the filtrated water was clear and completely colorless. Next, TW was washed with distilled water and was oven dried for 48 h at 70°C. Subsequently, the dried TW was crushed with a knife mill and sieved to achieve a mesh size between 125 and 250 μm. The prepared sample was stored in a plastic bottle for further use. No other chemical or physical treatments were applied prior to adsorption experiments.

2.3. Experimental setup

The fixed-bed column experiments were performed using a laboratory-scale glass column with an inner

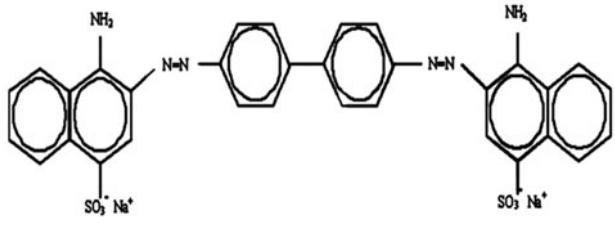

Fig. 1. Molecular structure of CR.

diameter of 1.4 cm and a height of 20 cm as shown in Fig. 2. Glass wool was placed at the top to retain the adsorbent as well as at the bottom of the adsorption column to better distribute the solution onto the medium surface. The column was packed with 6, 8, and 10 g of TW to obtain a particular bed height of adsorbent (equivalent to 8.9, 11.7, and 14.6 cm of bed depth). CR solution of known concentration (30, 40, and 50 mg/L) at pH 6 was pumped upward through the column by a peristaltic pump at a desired flow rate (4.6, 5.6, and 6.6 ml/min). Moreover, the CR concentration of 30 mg/l at the specific pH (4, 6, and 8) and the bed depth of 10 cm were examined. The pH of the solution was adjusted by adding 0.1 N NaOH and 0.1 N HCl solutions. The temperature of the influent feed was maintained at 30°C by means of a water circulation heater as shown in Fig. 2; in which water was passed through a surrounding jacket around the column. The effluent samples were collected at regular time intervals to determine the dye concentration in the solution. The dye concentration was measured using a UV–vis spectrophotometer (UNICAM, 8700 series, USA) at the wavelength of maximum absorbance (495 nm).

2.4. Column study

The point where the effluent concentration reaches arbitrarily at some low value is the breakthrough point (C_b) and the point where the concentration approaches to 90% of C_0 is considered the exhausted point of the adsorbent (C^*) [25]. The breakthrough point, breakthrough exhausted point, and the shape of the breakthrough curve are highly important characteristics of the operation, dynamic response, and process design of a sorption column [26]. The breakthrough curve is usually expressed by the ratio of effluent concentration (C_t) to influent concentration (C_0) (C_t/C_0) as a function of time (t). The effluent volume (V_{eff}) can be calculated as the following equation [26]:

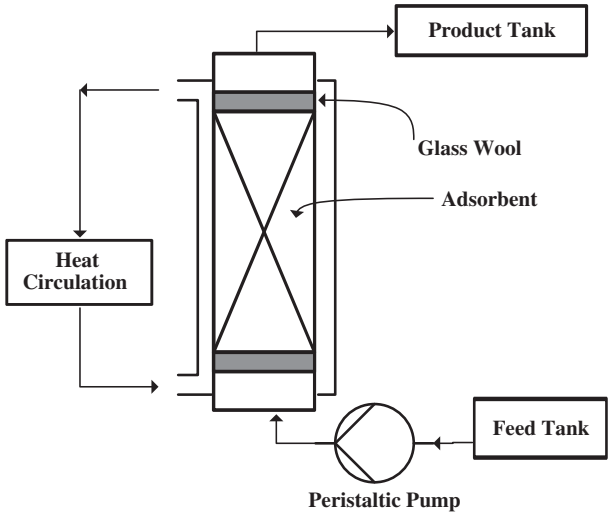

Fig. 2. Schematic diagram of the packed bed column apparatus.

$$V_{eff} = Qt_{total} \tag{1}$$

where t_{total} and Q represent the total flow time (min) and volumetric flow rate (ml/min). The total adsorbed CR quantity can be found from integrating the adsorbed concentration (C_{ad}) vs. t (min) plot which is the area under the breakthrough curves. The value of total adsorbed CR in the fixed-bed column for a given feed concentration and flow rate is calculated from Eq. (2) as reads [27]:

$$q_{total} = \frac{QA}{1,000} = \frac{Q}{1,000}\int_{t=0}^{t=t_{total}} C_{ad}\ dt \tag{2}$$

The equilibrium uptake (q_{eq}) or maximum column capacity in the column is defined by Eq. (3) as the total amount of adsorbed dye (q_{total}) per gram of adsorbent (W) at the end of total flow time [27]:

$$q_{eq} = \frac{q_{total}}{W} \tag{3}$$

The total influent CR entering the fixed-bed column (m_{total}) is obtained from the following equation [27,28]:

$$m_{total} = \frac{C_0 Q t_{total}}{1,000} \tag{4}$$

The flow rates represent the empty bed contact time (EBCT) on the column and can be calculated as [28]:

$$\text{EBCT (min)} = \text{bed volume (ml)} \ / \ \text{flow rate (ml/min)} \tag{5}$$

3. Results and discussion

3.1. The effect of different mass of adsorbents on the breakthrough curve

Fig. 3 illustrates the breakthrough curves for CR adsorption onto TW at different mass of adsorbents of

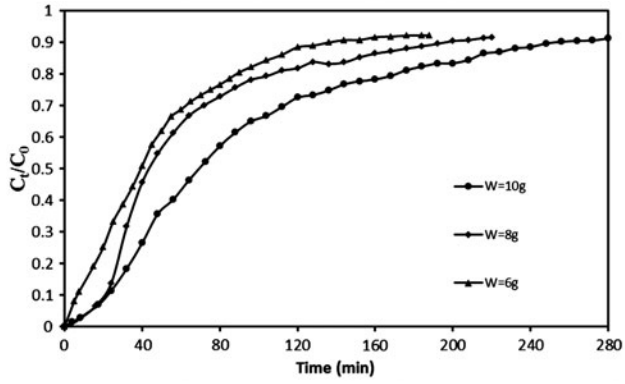

Fig. 3. The effect of different mass of the adsorbent on the breakthrough curves of CR adsorption on TW (inlet CR concentration = 30 mg/l, flow rate = 6.6 ml/min, temperature = 30°C, pH = 6).

6, 8, and 10 g (8.9, 11.7, and 14.6 cm), while other parameters such as flow rate, inlet concentration, and pH were kept constant at 6.6 ml/min, 30 mg/l, and 6, respectively. The experimental results are listed in Table 1. It is obvious from Fig. 3 that increasing the mass of the adsorbent, the exhaustion time was increased, since more binding sites were available for CR adsorption; besides, the slope of the breakthrough curves decreased with increasing of the mass of the adsorbent and more broadened mass transfer zone were achieved. As the mass of the adsorbent was increased from 6 to 10 g, the breakthrough point increased from 8.1 to 23.8 min. The increase of breakthrough point with bed depth can be attributed to the fact that by increasing the mass of the adsorbent, adsorption sites were increased. According to Table 1, the dye uptake capacity was significantly affected by the mass of the adsorbent. The values of total adsorbed CR were 10.62, 13.94, and 17.83 mg/g at different mass of the adsorbent of 6, 8, and 10 g, respectively. This can be interpreted by the fact that higher mass of the adsorbent provided more contact time of CR with TW adsorbent [29–31].

3.2. The effect of flow rate on the breakthrough curve

The effect of various flow rates (4.6, 5.6, and 6.6 ml/min) on the adsorption breakthrough curves of CR is shown in Fig. 4 by maintaining the constant mass of the adsorbent of 10 g, the inlet concentration of 30 mg/l, and pH of 6. It is evident that as the flow rate was increased, the steepness of breakthrough curve increased. This is ascribed to the fact that at a high rate of influent, there was not sufficient time for CR to contact with TW, hence the removal of CR decreased. In addition, by increasing the flow rate from 4.6 to 6.6 ml/min, the breakthrough point decreased from 27.8 to 23.8 min. At lower influent flow rate, the breakthrough time reaching saturation was significantly increased, which is due to the fact that at a low flow rate, CR molecules in dye solution had more time to be in contact with TW particles and the residence time in column increased which resulted in higher removal efficiency. The impact of the influent flow rate was considered on dye uptake capacity as well; the maximum dye uptake capacities were 3.00, 2.32, and 1.78 mg/g for flow rates of 4.6, 5.6, and 6.6 ml/min, respectively (Table 1). The increase in adsorption capacity with the decrease of the flow rate suggests that the adsorption process was controlled by intraparticle diffusion. The results were in agreement with other researchers [27,29,30].

3.3. The effect of inlet CR concentration on the breakthrough curve

The effect of different inlet CR concentration was investigated at three inlet concentration 30, 40, and 50 mg/l. Other operational parameters such as effluent flow rate, mass of adsorbent, and pH were unchanged

Table 1
The parameters of the fixed-bed column for the CR sorption onto TW at different conditions

C_0 (mg/l)	Q (ml/min)	W (g)	pH	t_b (min)	V_{eff} (ml)	m_{total} (mg)	q_{tot} (mg)	q_e (mg/g)	EBCT (min)
30	6.6	6	6	8.1	1,108.4	33.26	10.62	1.77	2.075
30	6.6	8	6	21.7	1,452	43.56	13.94	1.74	2.728
30	6.6	10	6	23.8	1,848	55.44	17.83	1.78	3.404
30	4.6	10	6	27.8	2,116	63.46	29.99	3.00	8.23
30	5.6	10	6	25.0	2,016	60.48	23.19	2.32	6.76
40	6.6	10	6	20.6	1,636.8	62.30	20.90	2.09	3.404
50	6.6	10	6	6.04	1,557.6	77.88	21.47	2.15	3.404
30	6.6	10	4	31.2	2,164.8	64.94	24.27	2.43	3.404
30	6.6	10	8	29.0	1,636.8	49.10	17.71	1.77	3.404

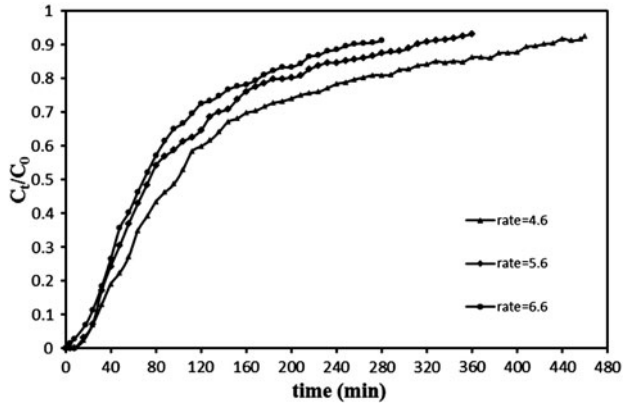

Fig. 4. The effect of different flow rates on the breakthrough curves of CR adsorption on TW (inlet CR concentration = 30 mg/l, mass of the adsorbent = 10 g, temperature = 30˚C, pH = 6).

at 6.6 ml/min, 10 g, and 6, respectively. Fig. 5 shows the breakthrough curves at various inlet concentrations. It can be observed that lower inlet concentration gave a later breakthrough curve and greater treated volume was obtained. At higher adsorbate concentration, sharper breakthrough curves were obtained, which is due to the fact that higher initial concentration provided greater driving force which resulted faster CR transport. As expected, the breakthrough point significantly decreased from 23.8 to 6.04 min by increasing the inlet concentration from 30 to 50 mg/l. This can be ascribed to higher initial concentration, which provided higher CR loading rates for the adsorbent sites; hence, the binding sites were occupied more quickly at higher initial concentration and smaller mass transfer zone were achieved [32,33]. The dye uptake capacity was increased with increasing the inlet concentration (Table 1), since higher initial concentration provided higher driving force against the CR transfer resistances for the adsorption process. Similar results have been found by other researchers [27,32,33].

3.4. The effect of initial pH solution on the breakthrough curve

pH value is an important process parameter which affects the adsorption uptake considerably. The breakthrough curves were applied to investigate the effect of pH of the influent on the adsorption of CR on TW for different pH of 4, 6, and 8 with a constant mass of adsorbent of 10 g, the inlet concentration of 30 mg/l, and the flow rate of 6.6 ml/min (Fig. 6). Similar steepness was observed for the breakthrough curves of various inlet solution pH. The breakthrough curves occurred more slowly for lower inlet solution pH, in which more treated volume was achieved. By increasing the inlet solution pH, the CR uptake capacity was decreased. Several mechanisms may have interfered in the adsorption process which may have impressive effects at different pH of the solution. The commonest mechanism, the electrostatic interaction, has been reported in many research studies. Lower pH values led to the increase of the H^+ ions in the inlet solution and TW attained the positive charge; accordingly, at lower pH, there existed an electrostatic attraction between the positively charged surface of the adsorbent and the anionic dye (CR). At higher pH, the negatively charged surface sites on the adsorbent made an electrostatic repulsion which did not favor the adsorption of CR onto TW. In addition, lower

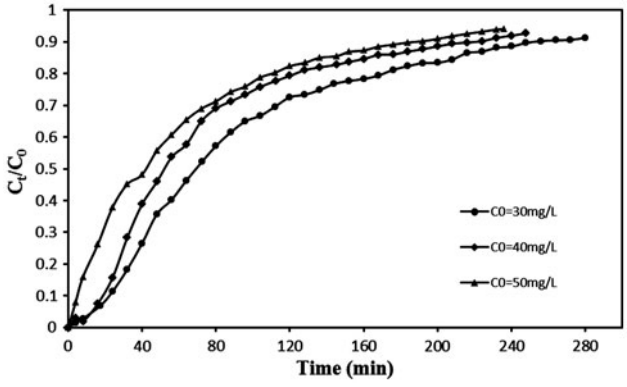

Fig. 5. The effect of inlet CR concentration on the breakthrough curves of CR adsorption on TW (flow rate = 6.6 ml/min, mass of the adsorbent = 10 g, temperature = 30˚C, pH = 6).

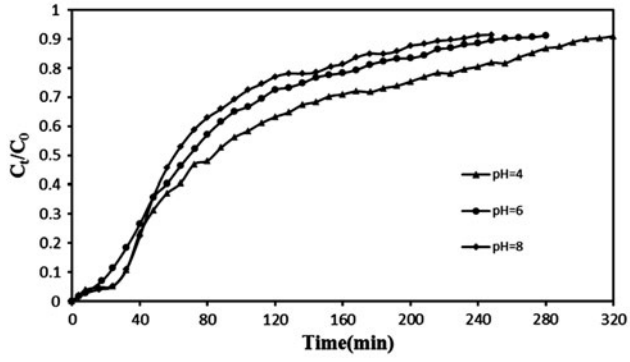

Fig. 6. The effect of inlet solution pH on the breakthrough curves of CR adsorption on TW (inlet CR concentration = 30 mg/l, flow rate = 6.6 ml/min, mass of the adsorbent = 10 g, temperature = 30˚C).

uptake of CR at higher pH was probably due to the competition between OH^- and dye anions for the positive sites on the adsorbent.

3.5. Characterization of TW

Fig. 7(a) and (b) show the SEM micrographs of TW before and after CR sorption. It can be seen from Fig. 7 that there existed highly heterogeneous pores within the TW particles. The dye-loaded TW particle can also be seen from the following figures.

3.6. Dynamic modeling of the breakthrough curves

The breakthrough models can be taken into practice to predict the concentration-time profiles in order to have a better design for the adsorption process. Several mathematical models have been developed to describe the column experiments [30,31]. Amongst them, the commonest model, including the Thomas, Adams–Bohart, Yoon–Nelson, and BDST models were used to predict the adsorption breakthrough curves.

3.6.1. The Adams–Bohart model

Adams and Bohart proposed a model based on the surface reaction theory, which assumes the adsorption rate as a function of both the residual capacity of the adsorbent and the concentration of adsorbate species. This model was applied for the description of initial parts of breakthrough curves [21,28,34]. The Adams–Bohart equation can be expressed as:

$$\ln\left(\frac{C_t}{C_0}\right) = k_{AB}C_0 t - k_{AB}N_0\frac{Z}{U_0} \tag{6}$$

where C_0 and C_t (mg/l) stand for the inlet and effluent dye concentration, k_{AB} (l/mg min) is designated as the rate coefficient, U_0 (cm/min) represents the linear velocity defined as the volumetric flow rate to the cross-sectional area of column bed, Z (cm) is the bed height, and N_0 (mg/l) stands for the sorption capacity of the adsorbent per unit volume of the bed. A linear plot of $\ln(C_t/C_0)$ vs. t was employed for the adsorption experimental data ranging from 0 to 0.5 in order to determine the model parameters k_{AB} and N_0 (the figure is not shown). These parameters can be calculated from the intercept and the slope of the plot. The values of the k_{AB} and N_0 for all of the breakthrough curves are presented in Table 2, as well as the corresponding correlation coefficient of the model. According to Table 2, the values of k_{AB} decreased with the increase of and inlet concentration, but it increased with flow rate. The values of correlation coefficient are at about 0.9 which represents the suitability of the model for the description of the breakthrough curves at the early parts of the adsorption.

3.6.2. Thomas model

The Thomas model is one of the commonly used models to describe the adsorption dynamic in the fixed-bed column. This model is based on the assumption that the flow in the column bed obeys the plug flow behavior and the Langmuir isotherm is considered for equilibrium. The nonlinear correlation

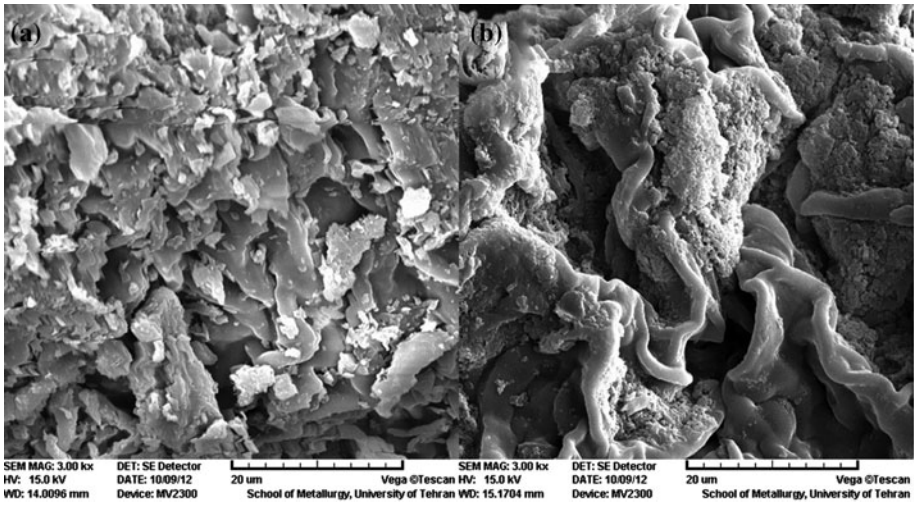

Fig. 7. SEM images for TW, and (a) before adsorption (b) after adsorption.

Table 2
Adams–Bohart model parameters at different conditions using linear regression analysis

Inlet concentrations (mg/l)	Flow rate (ml/min)	Mass of adsorbent (g)	pH	Adams–Bohart model		
				k_{AB} (l/mg min) × 10^4	N_0 (mg/l) × 10^{-2}	R^2
30	6.6	6	6	1.45	7.74	0.95
30	6.6	8	6	3.17	5.19	0.92
30	6.6	10	6	2.18	5.97	0.84
30	4.6	10	6	0.64	7.77	0.94
30	5.6	10	6	0.99	6.89	0.90
40	6.6	10	6	1.60	6.65	0.89
50	6.6	10	6	0.72	8.33	0.87
30	6.6	10	4	1.29	7.88	0.89
30	6.6	10	8	2.18	5.97	0.84

between concentration and time has been obtained, which is shown below [22,35]:

$$\frac{C_t}{C_0} = \frac{1}{1 + \exp(\frac{k_{Th} q_0 W}{Q} - k_{Th} C_0 t)} \quad (7)$$

The linearized form of the Thomas model is given as:

$$\ln\left(\frac{C_0}{C_t} - 1\right) = \frac{k_{Th} q_0 W}{Q} - k_{Th} C_0 t, \quad (8)$$

where Q (ml/min) is the flow rate, W (g) is the weight of adsorbent, k_{Th} (l/mg min) is the Thomas rate constant, and q_0 (mg/g) implies the maximum capacity of the adsorbent. A linear plot of $\ln[(C_0/C_t)-1]$ against t determined the values of the model parameters k_{Th} and q_0 from the intercept and the slope of the plot (the figure is not shown).

The relative constants along with the correlation coefficient of the model are presented in Table 3. From Table 3, it is evident that by increasing the bed depth, the values of k_{Th} decreased, while the values of q_0 increased. The values of k_{Th} increased with the increase of flow rate. This result suggests that the Thomas model was suitable for the adsorption processes where the external and internal diffusion was not the limiting step [28,36].

3.6.3. The Yoon–Nelson Model

The Yoon–Nelson model is based on the assumption that the rate of decrease in probability of adsorption for each adsorbate molecule is proportional to the probability of adsorbate adsorption and the probability of adsorbate breakthrough on the adsorbent [23,34,37]. The linearized form of the Yoon–Nelson model regarding to a single-component system is expressed as:

Table 3
Thomas model parameters at different conditions using linear regression analysis

Inlet concentrations (mg/l)	Flow rate (ml/min)	Mass of adsorbent (g)	pH	Thomas model		
				k_{Th} (ml/min mg) × 10^3	q_0 (mg/g)	R^2
30	6.6	6	6	1.317	1.51	0.94
30	6.6	8	6	0.920	1.46	0.75
30	6.6	10	6	0.770	1.71	0.90
30	4.6	10	6	0.433	1.57	0.88
30	5.6	10	6	0.510	1.57	0.89
40	6.6	10	6	0.688	1.82	0.82
50	6.6	10	6	0.454	1.73	0.85
30	6.6	10	4	0.707	2.15	0.81
30	6.6	10	8	0.897	1.70	0.78

$$\ln\left(\frac{C_t}{C_0 - C_t}\right) = k_{YN}t - \tau k_{YN} \quad (9)$$

where k_{YN} (1/min) is the rate constant and τ (min) is the time required for 50% of adsorbate breakthrough. The values of k_{YN} and τ can be calculated from the intercept and the slope of the linear plot of $\ln[C_t/(C_0-C_t)]$ vs. t based on Eq. (9) (the figure is not shown). The values of the model parameters k_{YN} and τ together with the correlation coefficient values are given in Table 4.

From Table 4, it can be seen that with the increase of bed depth, the values of k_{YN} decreased, while the values of τ increased. With the inlet CR concentration increasing, the value of τ significantly decreased, which is consistent with the fact that higher initial concentration provided greater driving force and led to faster saturation time. It can be concluded from Tables 3 and 4 that both the Thomas and Yoon–Nelson models provided an appropriate fit to experimental data according to relatively high correlation coefficient related to each model.

3.6.4. The bed depth service time model (BDST)

Hutchins developed the BDST model for predicting the relationship between the service time (t) and the bed depth (Z) in terms of the adsorption parameters. The BDST model is based on the assumption that the adsorbate is adsorbed onto the adsorbent surface directly and the intraparticle mass transfer resistance and the external film resistance are ignored in this model. On the other hand, this model assumes the surface reaction between the adsorbent and adsorbate in the solution [24,34]. The BDST model is defined as:

$$\ln\left(\frac{C_0}{C_t} - 1\right) = \ln\left(\exp\left(\frac{K_a N_0 Z}{u}\right) - 1\right) - K_a C_0 t \quad (10)$$

where K_a (l/mg min) represents the rate constant of BDST model and the other parameters are defined as before. Eq. (10) may be rearranged for linearized data plotting as:

$$t_b = \frac{N_0}{C_0 F} - \frac{1}{K_a C_0}\ln\left(\frac{C_0}{C_t} - 1\right) \quad (11)$$

Plots of t vs. Z at different values of C_t/C_0 0.1, 0.2, 0.3, and 0.4 are shown in Fig. 8. The values of the rate constant (K_a) and the average adsorption capacity per volume of bed (N_0) can be evaluated according to the slopes and the intercepts of the plots and the results are presented in Table 5, as well as the correlation coefficient of the BDST model. The equation of the BDST curves can be expressed in the form $y = ax+b$, where x and y imply the service time and the bed depth, respectively, and a and b can be calculated as:

$$a = \frac{N_0}{C_0 F} \quad (12)$$

and

$$b = \frac{1}{K_a C_0}\ln\left(\frac{C_0}{C_t} - 1\right) \quad (13)$$

The BDST model constants can be helpful to scale up the process for other flow rates and the concentration without further experimental runs. In the case of other flow rates and influent concentrations, the desired BDST equation can simply be established by the new

Table 4
Yoon–Nelson model parameters at different conditions using linear regression analysis

Inlet concentrations (mg/l)	Flow rate (ml/min)	Mass of adsorbent (g)	pH	Yoon–Nelson model		
				k_{YN} (1/min) × 10^2	τ(min)	R^2
30	6.6	6	6	3.87	46.021	0.94
30	6.6	8	6	2.76	59.091	0.75
30	6.6	10	6	2.31	86.455	0.90
30	4.6	10	6	1.30	81.569	0.88
30	5.6	10	6	1.53	93.680	0.89
40	6.6	10	6	2.75	69.011	0.82
50	6.6	10	6	2.27	52.568	0.85
30	6.6	10	4	1.80	142.172	0.76
30	6.6	10	8	2.69	77.446	0.78

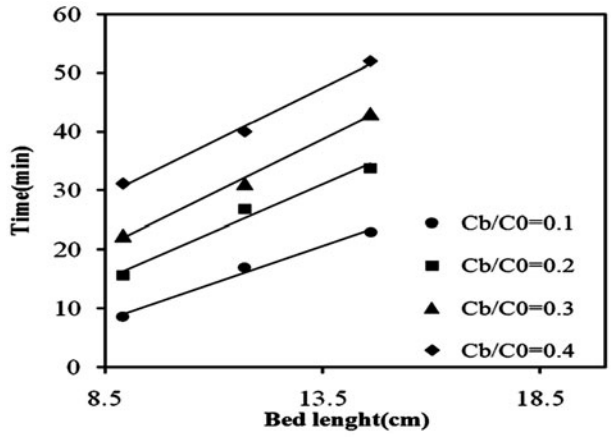

Fig. 8. BDST plots for 0.1, 0.2, 0.3, and 0.4 breakthrough for different bed depths (inlet CR concentration = 30 mg/l, flow rate = 6.6 ml/min, temperature = 30°C).

Table 5
The calculated constants of BDST model for the adsorption of CR in fixed-bed column (inlet CR concentration = 30 mg/l, flow rate = 6.6 ml/min, temperature = 30°C)

C_t/C_0	a (min/cm)	b (min)	K_a (l/mg min)	N_0 (mg/l) × 10^2	R^2
0.1	2.516	−12.08	0.006099	4.98	0.86
0.2	3.188	−12.01	0.008172	6.31	0.98
0.3	3.63	−10.41	0.010782	7.20	0.99
0.4	4.349	−10.19	0.011978	8.61	0.89

slopes and intercepts based on the former calculated ones [34,36].

From Table 5, with the increase of C_t/C_0, both the values of the adsorption capacity, N_0, and the rate constant, K_a, increased. It can be seen from Fig. 8 that the BDST plots fitted the experimental data properly. According to the Table 5, the correlation coefficient values in the range from 0.86 to 0.99, confirmed the validity of the BDST model for the adsorption of CR onto TW in the fixed-bed column.

4. Conclusion

In this study, TW has been identified as a promising adsorbent for the removal of CR from aqueous solution using a fixed-bed column. It was found that higher mass of the adsorbent, lower flow rate, and lower influent concentration would be in favor of the adsorption process. Furthermore, the solution pH values significantly affected the adsorption of CR, in which the adsorption process performed better at lower pH values. Both the Thomas and Yoon–Nelson models sufficiently predicted the breakthrough curves at all the experimental conditions. Moreover, the column data were fitted to the BDST model with a correlation coefficient of $R^2 \geq 0.86$ at different conditions.

References

[1] G. Crini, Non-conventional low-cost adsorbents for dye removal: A review, Bioresour. Technol. 97 (2006) 1061–1085.
[2] M.A.M. Salleh, D.K. Mahmoud, W.A. Karim, A. Idris, Cationic and anionic dye adsorption by agricultural solid wastes: A comprehensive review, Desalination 280 (2011) 1–13.
[3] I.M. Banat, P. Nigam, D. Singh, R. Marchant, Microbial decolorization of textile-dyecontaining effluents: A review, Bioresour. Technol. 58 (1996) 217–227.
[4] K.Y. Foo, B.H. Hameed, An overview of dye removal via activated carbon adsorption process, Desalin. Water Treat. 19 (2010) 255–274
[5] A.H. Sulaymon, W.M. Abood, Removal of reactive yellow dye by adsorption onto activated carbon using simulated wastewater, Desalin. Water Treat. 52 (2014) 3421–3431.
[6] R. Ertaş, N. Öztürk, Removal of lead from aqueous solutions by using chestnut shell as an adsorbent, Desalin. Water Treat. 51 (2013) 2903–2908.
[7] Z. Hu, H. Chen, F. Ji, S. Yuan, Removal of Congo Red from aqueous solution by cattail root, J. Hazard. Mater. 173 (2010) 292–297.
[8] S. Dawood, T.K. Sen, Removal of anionic dye congo red from aqueous solution by raw pine and acid-treated pine cone powder as adsorbent: Equilibrium, thermodynamic, kinetics, mechanism and process design, Water Res. 46 (2012) 1933–1946.
[9] A. Tor, Y. Cengeloglu, Removal of congo red from aqueous solution by adsorption onto acid activated red mud, J. Hazard. Mater. 138 (2006) 409–415.
[10] S. Wang, Y. Boyjoo, A. Choueib, Z.H. Zhu, Removal of dyes from aqueous solution using fly ash and red mud, Water Res. 39 (2005) 129–138.
[11] E. Unuabonah, B. Olu-Owolabi, E. Fasuyi, K. Adebowale, Modeling of fixed-bed column studies for the adsorption of cadmium onto novel polymer–clay composite adsorbent, J. Hazard. Mater. 179 (2010) 415–423.
[12] C. Li, P. Champagne, Fixed-bed column study for the removal of cadmium (II) and nickel (II) ions from aqueous solutions using peat and mollusk shells, J. Hazard. Mater. 171 (2009) 872–878.
[13] S. Singh, V. Srivastava, I. Mall, Fixed-bed study for adsorptive removal of furfural by activated carbon, Colloids Surf., A 332 (2009) 50–56.
[14] G. Vázquez, R. Alonso, S. Freire, J. Gonzalezalvarez, G. Antorrena, Uptake of phenol from aqueous solutions by adsorption in a Pinus pinaster bark packed bed, J. Hazard. Mater. 133 (2006) 61–67.
[15] M. Foroughi-dahr, H. Abolghasemi, M. Esmaili, A. Shojamoradi, H. Fatoorehchi, Adsorption characteristics of congo red from aqueous solution onto tea waste, Chem. Eng. Commun. 202 (2014) 181–193.

[16] B. Amarasinghe, R. Williams, Tea waste as a low cost adsorbent for the removal of Cu and Pb from wastewater, Chem. Eng. J. 132 (2007) 299–309.
[17] E. Khosla, S. Kaur, P.N. Dave, Tea waste as adsorbent for ionic dyes, Desalin. Water Treat. 51 (2013) 34–36.
[18] M.K. Mondal, Removal of Pb(II) ions from aqueous solution using activated tea waste: Adsorption on a fixed-bed column, J. Environ. Manage. 90 (2009) 3266–3271.
[19] E. Malkoc, Y. Nuhoglu, Removal of Ni(II) ions from aqueous solutions using waste of tea factory: Adsorption on a fixed-bed column, J. Hazard. Mater. 135 (2006) 328–336.
[20] E. Malkoc, Y. Nuhoglu, Fixed bed studies for the sorption of chromium(VI) onto tea factory waste, Chem. Eng. Sci. 61 (2006) 4363–4372.
[21] G.S. Bohart, E.Q. Adams, Some aspects of the behavior of charcoal with respect to chlorine, J. Chem. Soc. 42 (1920) 523–544.
[22] H.C. Thomas, Heterogeneous ion exchange in a flowing system, J. Am. Chem. Soc. 66 (1944) 1664–1666.
[23] Y.H. Yoon, J.H. Nelson, Application of gas adsorption kinetics I. A theoretical model for respirator cartridge service life, Am. Ind. Hyg. Assoc. J. 45 (1984) 509–516.
[24] R.A. Hutchins, New method simplifies design of activated carbon systems, Chem. Eng. 80 (1973) 133–138.
[25] C. Valderrama, J. Arévalo, I. Casas, M. Martínez, N. Miralles, A. Florido, Modelling of the Ni(II) removal from aqueous solutions onto grape stalk wastes in fixed-bed column, J. Hazard. Mater. 174 (2010) 144–150.
[26] Z. Aksu, Ş.Ş. Çağatay, F. Gönen, Continuous fixed bed biosorption of reactive dyes by dried *Rhizopus arrhizus*: Determination of column capacity, J. Hazard. Mater. 143 (2007) 362–371.
[27] F. Gönen, Z. Aksu, A comparative adsorption/biosorption of phenol to granular activated carbon and immobilized activated sludge in a continuous packed bed reactor, Chem. Eng. Commun. 190 (2003) 763–778.
[28] S. Chen, Q. Yue, B. Gao, Q. Li, X. Xu, K. Fu, Adsorption of hexavalent chromium from aqueous solution by modified corn stalk: A fixed-bed column study, Bioresour. Technol. 113 (2012) 114–120.
[29] A.H. Sulaymon, D.W. Abbood, A.H. Ali, Removal of phenol and lead from synthetic wastewater by adsorption onto granular activated carbon in fixed bed adsorbers: Prediction of breakthrough curves, Desalin. Wat. Treat. 40 (2012) 244–253.
[30] E. Malkoc, Y. Nuhoglu, Removal of Ni(II) ions from aqueous solutions using waste of tea factory: Adsorption on a fixed-bed column, J. Hazard. Mater. 135 (2006) 328–336.
[31] K. Vijayaraghavan, J. Jegan, K. Palanivelu, M. Velan, Removal of nickel(II) ions from aqueous solution using crab shell particles in a packed bed up flow column, J. Hazard. Mater. 113 (2004) 223–230.
[32] M. Mukhopadhyay, T. Kaur, R. Khanna, Fixed bed and reduced lumped diffusion model parameter estimation of copper biosorption using *Aspergillus niger* biomass, Can. J. Chem. Eng. 90 (2012) 1011–1016.
[33] J. Goel, K. Kadirvelu, C. Rajagopal, V. Kumar Garg, Removal of lead(II) by adsorption using treated granular activated carbon: Batch and column studies, J. Hazard. Mater. 125 (2005) 211–220.
[34] H. Patel, R.T. Vashi, Fixed bed column adsorption of ACID Yellow 17 dye onto Tamarind Seed Powder, Can. J. Chem. Eng. 90 (2012) 180–185.
[35] F. Rozada, M. Otero, A.I. García, A. Morán, Application in fixed-bed systems of adsorbents obtained from sewage sludge and discarded tyres, Dyes Pigm. 72 (2007) 47–56.
[36] R. Han, Y. Wang, X. Zhao, Y. Wang, F. Xie, J. Cheng, M. Tang, Adsorption of methylene blue by phoenix tree leaf powder in a fixed-bed column: Experiments and prediction of breakthrough curves, Desalination 245 (2009) 284–297.
[37] Z. Aksu, F. Gönen, Biosorption of phenol by immobilized activated sludge in a continuous packed bed: Prediction of breakthrough curves, Process Biochem. 39 (2004) 599–613.